JOURNAL OF MATERIALS SCIENCE 9 (1974) 245–257

Deformation of internal boundaries

K. SADANANDA, M. J. MARCINKOWSKI
Engineering Materials Group and Department of Mechanical Engineering, University of Maryland, College Park, Maryland, USA

A geometrical analysis of the deformation of internal boundaries is presented using the slip systems as reference co-ordinate axes to describe the orientation of the two phases adjacent to the boundary. The present analysis can be applied to any type of boundary such as a grain boundary, a twin boundary or a two-phase interface. The nature of the disturbance left by a dislocation cutting through the boundary is characterized by a boundary dislocation, the Burgers vector of which can be determined from the orientation relationship between the adjacent slip systems. Whenever the crystal dislocation, cutting through the boundary, has a Burgers vector component normal to the boundary, the disturbance also possesses a ledge character, the motion of which may cause both grain boundary sliding as well as migration. The formulae derived are applied to simple cases to determine the nature of the boundary dislocations.

1. Introduction

Though many attempts have been made to establish the exact structure-property relationships for polycrystals during the past half century, an understanding of the detailed deformation mechanisms involved is quite limited. An extension of available knowledge obtained from the deformation of single crystals to polycrystals is very difficult owing to the imposition of additional constraints by the grain boundaries [1]. Much work has been done with bi-crystals [2-11] in order to understand the constraints imposed by the grain boundary on the deformation of the entire aggregate. It was observed that slip lines in many cases are continuous across the boundary [11]. Furthermore, additional slip systems were found to be activated in both grains (systems other than those which would operate had the crystals been deformed separately). The continuity of slip across the boundary implies that glide dislocations pass through the boundary and that the boundary itself undergoes deformation because of this passage. The ease with which the boundary undergoes deformation should control the ease with which slip can propagate from one grain to the other. The deformation of the boundaries separating two crystals of differing crystal structure is much more complicated. Studies of the deformation of mild steel fibres imbedded in a silver matrix [12] showed that slip lines were found to be continuous across the interface with slip lines propagating from silver to mild steel. Such composites with well-defined interfaces are produced by directional solidification of eutectic alloys [13, 14]. Fleischer [15] was the first to point out that a dislocation crossing into a region of different lattice constant along the slip direction must create a sessile dislocation at the interface. However, he considered a simple case where the slip systems in the two crystals were parallel. For a general case, deformation of the boundary is much more complicated.

The deformation of simple tilt and twist boundaries within simple cubic structures has been studied by passing dislocations across the boundaries [16-20]. The resulting disturbances at these boundaries were in turn analysed using the concept of grain-boundary dislocations [21-24]. In particular, the above studies covered several individual cases involving the passage of edge and screw dislocations across a symmetric tilt or twist boundary under conditions of both homogeneous [19] and heterogeneous shear [18]. In the present paper, a general analysis is presented which is applicable to any type of boundary including the interfaces contained within two-phase materials. In the first part of the present paper, general equations describing the shear of a general boundary are derived,

while in the latter sections, they are applied to some specific cases. The present analysis, however, neglects the nature of the initial dislocation structure of the boundary as well as the interaction of these structural dislocations with the dislocations shearing the boundary.

2. Generalized co-ordinates

For a complete mathematical description of a boundary separating two crystals, five parameters are necessary since such a boundary has five degrees of freedom [25]. It is customary to prescribe these parameters in terms of three Eulerian angles [26] which describe the rotation of the two grains and two angles to describe the orientation of the outward normal to the boundary*. For a consideration of the shear of the boundary by the passage of dislocations across it, it is sometimes more advantageous to prescribe the above five parameters in terms of the slip systems directly, instead of in terms of Eulerian angles. Both descriptions, however, are essentially the same.

Fig. 1a, for example, shows how the grain boundary is specified with respect to the two slip systems in adjacent grains. As an example, we have represented the boundary as an interface and the two crystals adjacent to the boundary as two phases which may have two different crystal structures. However, the boundary can also be a grain boundary or a twin boundary in which case the crystal structures of the two phases represented in Fig. 1a are the same. Hence, in the present analysis, terms such as phases and interface are used in a very general sense and the crystal structures of the two phases separated by the boundary may or may not be the same. It is assumed, further, that the predominant slip systems of the two phases are known.

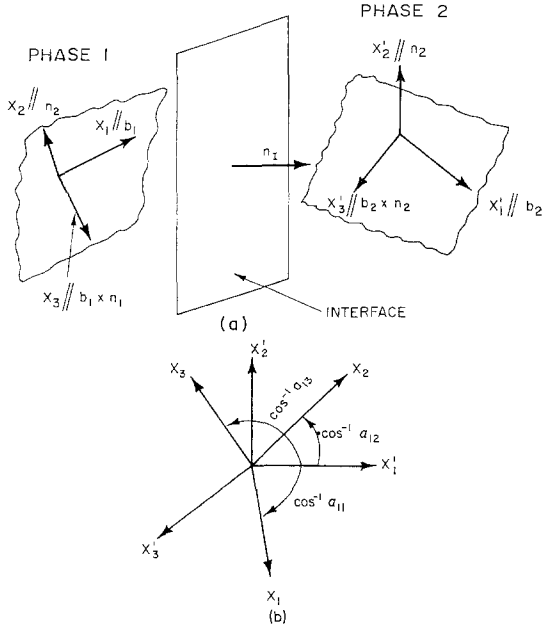

Figure 1 (a) Co-ordinate axes in two adjacent phases, (b) relationship between the two systems of co-ordinates.

The reference co-ordinates, $\mathbf{x}_1$, $\mathbf{x}_2$, $\mathbf{x}_3$ are chosen to be parallel to $\boldsymbol{b}_1$, $\mathbf{n}_1$ and $\boldsymbol{b}_1 \times \mathbf{n}_1$ respectively, where $\boldsymbol{b}_1$ is the Burgers vector and $\mathbf{n}_1$ is a vector normal to the slip plane in phase I. The co-ordinates $\mathbf{x}_1'$, $\mathbf{x}_2'$, $\mathbf{x}_3'$ correspond to $\boldsymbol{b}_2$, $\mathbf{n}_2$ and $\boldsymbol{b}_2 \times \mathbf{n}_2$ respectively, where $\boldsymbol{b}_2$ and $\mathbf{n}_2$ specify the slip system in phase II. The outward normal to the boundary before deformation is denoted by $\mathbf{n}_I$. It is to be noted that unless otherwise mentioned, all of the vectors are expressed in terms of the unprimed co-ordinate system. Furthermore, in all of the following figures two vectors are indicated as parallel vectors by two inclined lines. The relation between the two systems of co-ordinates is shown in Fig. 1b. The transformation matrix that describes the primed system of co-ordinates in Fig. 1b with respect to the unprimed system of co-ordinates is given by

$$a = a_{ji} \qquad \Delta \qquad (1)$$

where a_{ji} are the directional cosines of the primed co-ordinate axes. Although the above matrix contains nine elements, it can be easily shown that only three of them are independent [28] and these correspond to the three Eulerian angles.

3. Propagation of slip across a boundary

Having described the boundary and the orientation of the adjacent crystals in terms of the two slip systems and the normal vector (Fig. 1) we will now describe its deformation. Fig. 2 schematically illustrates the passage of a dislocation from phase I to phase II. In general, the magnitude of the Burgers vector and the interplanar distances A and a need not be the same as indicated in Fig. 2. In such cases, the continuity

*Chalmers [27] considered additional degrees of freedom associated with the relaxed boundaries. For the purpose of the present geometrical analysis, it will suffice to consider only the five degrees of freedom discussed above.

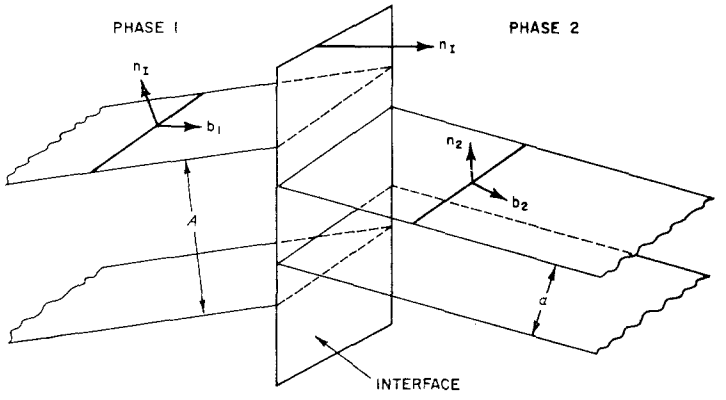

Figure 2 Passage of a dislocation from one phase into the other.

of slip planes across the interface is established by the presence of interface dislocations [16, 29].* Due to the relative rotation of the two slip systems as well as to the difference in the magnitude of the slip vectors, a disturbance is left at the boundary when a dislocation passes from one phase into the other. Such a disturbance is characterized by an effective Burgers vector given by

$$\boldsymbol{b}_I = (\boldsymbol{b}_1 - a\,\boldsymbol{b}_2) \tag{2}$$

and a line vector L_I which can be represented, for simplicity, by

$$L_I = L_1 + L_2 \tag{3}$$

where $\mathbf{L}_1$ and $\mathbf{L}_2$ are the lines of intersection of the two slip planes adjacent to the boundary with the boundary plane. Here subscripts 1 and 2 refer to phases I and II, respectively, while subscript I refers to the interface plane. By definition, the dislocation described by Equations 2 and 3 is glissile if its Burgers vector and line vector lie in the plane of the boundary.† This condition can be expressed as

$$\boldsymbol{b}_I \cdot \mathbf{n}_I = 0\ . \tag{4}$$

The dislocation will be sessile otherwise.

There could, however, be cases where the crystal lattice dislocations (CLD) may not cut through the boundary, but become embedded in the boundary. In such cases, the dislocations can still be considered as interface dislocations where Burgers vectors are given by Equation 2 with $\boldsymbol{b}_1$ or $\boldsymbol{b}_2$ equal to zero depending upon whether the CLD belongs to phase I or phase II. Since Equation 2 is based only on the principle of conservation of Burgers vector for a dislocation, it does not depend on whether the CLD arrive at the boundary by glide or by climb.

As a result of the shear, the boundary itself undergoes shape and orientation changes which can be determined from the geometrical properties of the dislocation responsible for the shear. For example, when a dislocation with Burgers vector $\boldsymbol{b}_1$ cuts through the boundary, it leaves a ledge in the boundary, the component of its height normal to the boundary is given by

$$h_1 = \frac{(\boldsymbol{b}_1 \,.\, \boldsymbol{n}_I) + (\boldsymbol{b}_2 \,.\, \boldsymbol{n}_I)}{2}\ . \tag{5}$$

In cases where the ledges are formed in the boundary, the ledges and their associated dislocation are to be considered as one entity since one cannot be separated from the other [31, 32]. Owing to its dislocation character, the boundary ledge can be classified as either a glissile or glide ledge or as a sessile or climb ledge [33] on the basis of Equation 4. Whenever the ledge moves, either by glide or by climb, the boundary undergoes migration. Boundary sliding could also occur along with migration if the dislocations associated with the ledge have Burgers vector components parallel to the boundary [32]. Many experimental observations [34-37], in fact, show that grain-boundary sliding almost always occurs along with grain-boundary migration.

*These interface dislocations have long range stress fields associated with them. Such long range stress fields are generally relieved by the presence of appropriate misfit dislocations in either phase [30]. For the purpose of the present analysis, however, we assume that there is a continuity of slip planes across the boundary whenever the slip plane traces at the boundary are parallel (Fig. 2).
†Since the Burgers vector $\boldsymbol{b}_I$ is not in general a lattice vector of either phase, the mobility, if any, of the mismatch is restricted to the plane of the interface.

The displacement of the boundary as a result of its migration owing to the motion of the ledge is given by the component of the height of the ledge normal to the boundary, h_1 (Equation 5). On the other hand, the magnitude of the sliding is given by the magnitude of the component of the Burgers vector of the interface dislocation parallel to the boundary, i.e., by

$$\mathbf{h}_2 = \boldsymbol{b}_\mathrm{I} - (\boldsymbol{b}_\mathrm{I} \,.\, \mathbf{n}_\mathrm{I})\mathbf{n}_\mathrm{I} \qquad (6)$$

The ratio of $|\,\mathbf{h}_2\,|$ to h_1 gives the ratio of the boundary sliding to its migration as a result of the motion of the ledge. For grain boundaries, it is possible to represent Equation 2 in terms of a co-ordinate system that describes a common lattice between the two grains, such as the coincidence site lattice or its sublattice [31] (SCS lattice). In terms of the SCS lattice all Burgers vectors, such as $\boldsymbol{b}_1$, $\boldsymbol{b}_2$ and $\boldsymbol{b}_\mathrm{I}$ are expressible in integral units. In such cases the ratio of brain-boundary sliding to its migration is expressible in terms of integer ratios. On the other hand, if the dislocations do not have ledge character, and if they are still glissile (Equation 4) then their motion on the plane of the interface causes pure sliding.

4. Homogeneous shear

As discussed previously [16] the passage of equal numbers of dislocations from one phase to the other on every Mth plane causes a homogeneous shear of the boundary. The shape and orientation changes that occur as a result of the homogeneous shear are schematically illustrated in Fig. 3. The ledges associated with the homogeneous shear are represented in Fig. 3b. If A′B′C′D′ represents an average plane of the boundary after shear and $\mathbf{N}_\mathrm{I}$ its outward normal, then the change in the orientation of the plane of the boundary as a result of the homogeneous shear can be represented by

$$\tan\phi = \frac{Nh_1}{M} \qquad (7a)$$

and

$$\mathbf{N}_\mathrm{I} = \cos\phi\,\mathbf{n}_\mathrm{I} - \sin\phi\,(\mathbf{L}_\mathrm{I} \times \mathbf{n}_\mathrm{I}) \qquad (7b)$$

where N is the number of dislocations cutting through the boundary on every Mth plane, and h_1 from Equation 5 is the height of the ledge owing to each dislocation. For $h_1 = 0$, corresponding to the case where the cutting dislocations do not form ledges in the boundary, $\phi = 0$ from Equation 7, as is to be expected. In such cases, the boundary orientation remains unaltered.

Fig. 3c also shows the array of interface dislocations that are left in the boundary as a result of the homogeneous shear. The Burgers vectors of these dislocations are given by Equation 2. This array can be resolved into three simpler arrays, namely, one screw dislocation array and two edge dislocation arrays, the stress fields of which have been explicitly calculated using an isotropic approximation [38]. The components of the Burgers vectors of

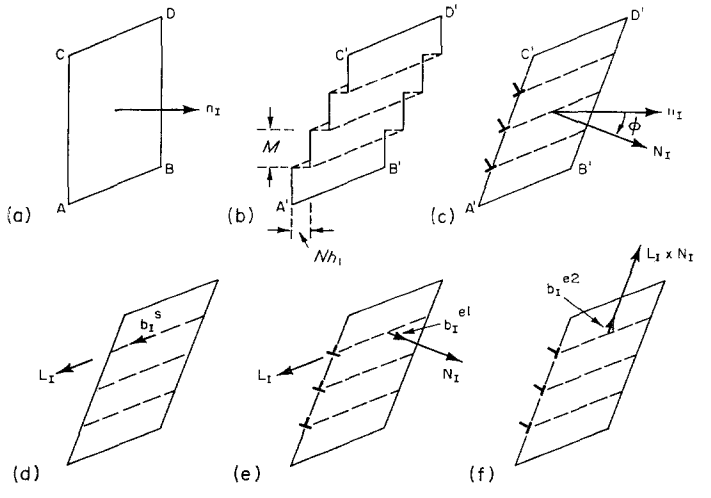

Figure 3 (a) Plane of the interface before shear, (b) ledges formed owing to homogeneous shear, (c) orientation of the average interface plane after shear, (d) (e) and (f) resolution of interface dislocations as pure screw and edge dislocations.

the dislocations in the simpler arrays (Fig. 3d, e, f) are given by

$$b_I^s = \boldsymbol{b}_I \,.\, \mathbf{L}_I \tag{8}$$

$$b_I^{e1} = \boldsymbol{b}_I \,.\, \mathbf{N}_I \tag{9}$$

$$b_I^{e2} = \boldsymbol{b}_I \,.\, (\mathbf{L}_I \times \mathbf{N}_I) \,. \tag{10}$$

The dislocation arrays d and f in Fig. 3, whose Burgers vectors are given by Equations 8 and 10, have long range stresses associated with them. The array of dislocations represented by Fig. 3e, on the other hand, has no long range stress fields. The array, however, changes the relative orientation of the two phases. In particular, it induces an additional tilt component $\Delta\theta$, the axis of the tilt being parallel to $\mathbf{L}_I$, the line vector of the dislocations.

If the boundary before shear possesses a tilt component, then the additional tilt angle, $\Delta\theta$, induced by the homogeneous shear could either increase or decrease the original tilt angle. In the approximation of a small homogeneous shear, the tilt component induced by the shear is given by [39]

$$\Delta\theta \approx \frac{|\boldsymbol{b}_I^{e1}|}{M} \,. \tag{11}$$

For further deformation of the boundary, the transformation matrix a_{ji} in Equation 1 should incorporate this change in the orientation of the two phases in order to determine the Burgers vector of the interface dislocation by Equation 2.

5. Effect of stress relief

The long range stress fields produced as a result of the homogeneous shear could, in general, be relieved by the nucleation of appropriate crystal lattice dislocations from both phases. The CLD react at the boundary to give the interface dislocations with Burgers vector components that are opposite to the ones produced during the deformation. They could increase the asymmetry, ϕ, in Fig. 3c by increasing the height of the ledges and also could restore the original misorientation angle θ. Some of these aspects are discussed in detail with reference to the structure of asymmetric tilt boundaries [40, 41]. It may not be possible, in general, to relieve the stress fields of all the dislocation arrays in Fig. 3 by one set of crystal lattice dislocations from both phases. Furthermore, stress relief could also occur without the nucleation of these crystal lattice dislocations, but with the rearrangement of the interface dislocations by both glide and climb into arrays that have no long range stress fields. For example, the dislocations in the array represented in Fig. 3f could move by glide and climb into the boundaries that are normal to the original boundary and form a tilt wall. Such a rearrangement, in addition to reducing the long range stress fields of the dislocation array in Fig. 3f, alters the misorientation relationships between the two phases adjacent to the boundaries in which they now exist [42]. In the later part of this paper, some of these processes are discussed with reference to the specific dislocation arrays generated as a result of homogeneous shear of the interface boundaries.

It was shown earlier that disclinations are necessary for the passage of edge dislocations across a twist boundary by glide [20]. For this case, the slip planes traces, $\mathbf{L}_1$ and $\mathbf{L}_2$ make an angle equal to the angle of twist at the boundary. In general, the conditions under which disclinations are necessary for the passage of dislocations across an interface, *precluding diffusion*, can be stated as follows. First, the slip vectors $\boldsymbol{b}_1$ and $\boldsymbol{b}_2$ should have a component parallel to the normal vector $\mathbf{n}_I$ of the boundary. This condition can be expressed as

$$\boldsymbol{b}_1 \,.\, \mathbf{n}_I \neq 0$$

and

$$\boldsymbol{b}_2 \,.\, \mathbf{n}_I \neq 0 \,. \tag{12}$$

Secondly, the traces of slip planes on the plane of the boundary should make an angle γ with one another as shown in Fig. 4. The above conditions will imply that the slip steps produced along the boundary will make an angle γ with one another and, hence, disclination loops are necessary to accommodate the mismatch at the boundary.

Since $\boldsymbol{b}_1$, $\boldsymbol{b}_2$ and $\mathbf{n}_I$ are selected parameters, the first condition can be readily checked. For the second condition, the angle γ should be determined. For this, the unit line vectors $\mathbf{L}_1$ and $\mathbf{L}_2$, which are the lines of intersection of the slip planes in phases I and II, respectively, with the plane of the interface (see Fig. 4), can be determined using the following relations:

$$\mathbf{L}_1 = \mathbf{n}_1 \times \mathbf{n}_I \tag{13}$$

and

$$\mathbf{L}_2 = \mathbf{n}_2' \times \mathbf{n}_I \tag{14}$$

where $\mathbf{n}_2'$ is the vector $\mathbf{n}_2$ expressed in terms of the unprimed co-ordinates using Equation 1. Thus

$$\mathbf{n}_{2i}' = a_{ij}\, \mathbf{n}_{2j}. \tag{15}$$

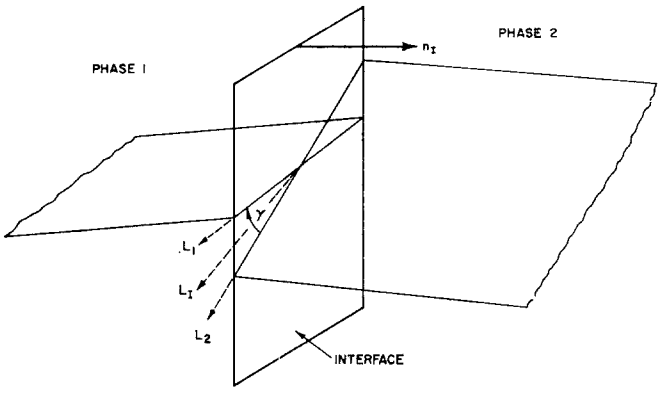

Figure 4 Orientation of the slip plane traces at an interface.

Equations 13 and 14 give $\mathbf{L}_1$ and $\mathbf{L}_2$ expressed in terms of unprimed co-ordinates. The angle γ (Fig. 4) is given by

$$\gamma = \cos^{-1}(\mathbf{L}_1 \,.\, \mathbf{L}_2) \,. \tag{16}$$

Thus, if $\gamma = 0$ twist disclinations are not necessary for the channelling of dislocations from one phase into the other; whereas, when $\gamma \neq 0$, disclinations are necessary if the Burgers vectors have a component along $\mathbf{n}_I$.

On the other hand, if diffusion is not precluded, the dislocations can cut through the boundary leaving behind a boundary dislocation given by Equation 2. Similarly, Equation 5 can be used to determine the height of the ledges generated as a result of such deformation.

Finally, Equation 2 could also be represented in any other system of co-ordinates. For example, if the orientation relationship between the two phases are given in terms of the co-ordinates of the unit cell of each crystal, then the transformation matrix a_{ij} that connects the slip systems in the two phases is given by

$$a_{ij} = S_{ik}\, C_{kl}\, S_{lj}' \tag{17}$$

where S_{ik} and S_{lj}' are the transformation matrices that connect the slip systems in phase I and phase II to the co-ordinates of the unit cells in the respective phases, while C_{kl} is the transformation matrix that connects the co-ordinates of the unit cells of the two phases. Fig. 5 schematically represents the order of these transformations.

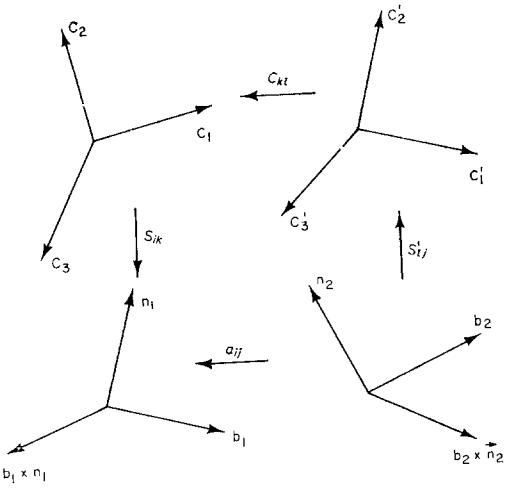

Figure 5 Transformation that relate the two slip systems adjacent to the interface.

6. Applications

In the following sections the above relations will be applied to the deformation of interfaces or grain boundaries. The passage of dislocations of simple orientation is considered below and the passage of dislocations comprising any complex configurations can be resolved into the simple orientation. It should be understood, however, that whenever a dislocation that has a Burgers vector component normal to the boundary passes through the boundary it leaves behind a ledge given by Equation 5 along with the boundary dislocation.

In a previous analysis [19] glide dislocations were described as parallel or perpendicular dislocations with reference to a rotation axis. Since both the rotation axis as well as the line vector of the dislocations are arbitrary in this analysis, we fix the line vector and change the rotation axis. The description of the dislocation as parallel or perpendicular still remains the

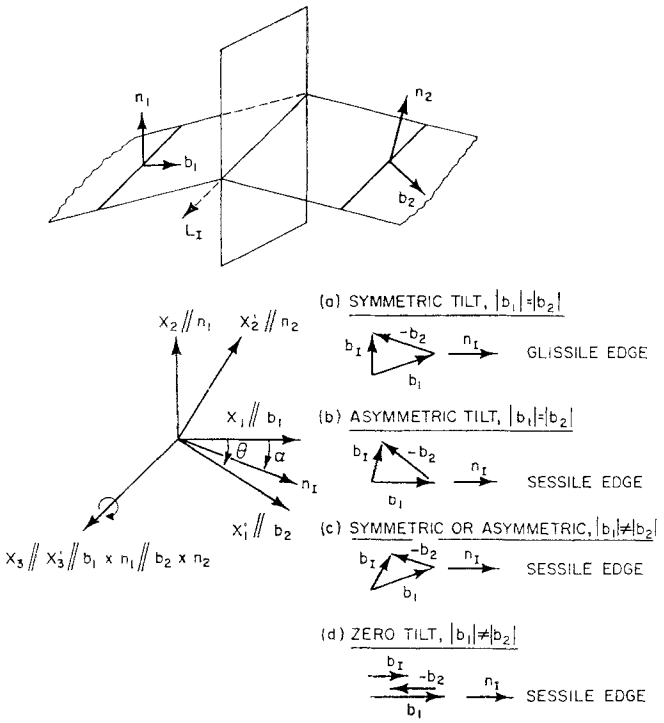

Figure 6 Passage of parallel edge dislocation from phase I to phase II and the characteristics of the resulting interface dislocations for various orientations of the slip systems adjacent to the boundary.

same. Furthermore, the orientation of $\boldsymbol{b}_2$ with reference to $\mathbf{L}_2$ is arbitrary, hence, the nature of the glide dislocation as it passes from phase I to phase II need not remain the same. The coordinate axes selected for all of the following examples are such that $\mathbf{x}_1$, $\mathbf{x}_2$ and $\mathbf{x}_3$ are parallel to $\boldsymbol{b}_1$, $\mathbf{n}_1$ and $\boldsymbol{b}_1 \times \mathbf{n}_1$, respectively, and $\mathbf{x}_1'$, $\mathbf{x}_2'$ and $\mathbf{x}_3'$ are parallel to $\boldsymbol{b}_2$, $\mathbf{n}_2$ and $\boldsymbol{b}_2 \times \mathbf{n}_2$, respectively. This selection is consistent with the general analysis presented earlier.

6.1. Edge dislocations

Consider the two slip systems in the two phases oriented with respect to each other by a rotation about the $\mathbf{x}_3$ axis as represented in Fig. 6. Owing to this rotation, the two slip planes are tilted with respect to one another by an angle θ. The orientation of $\mathbf{n}_I$ is represented by the angle α which is equal to $\theta/2$ for a symmetric tilt. Consider an edge dislocation parallel to the axis of rotation. When this edge dislocation passes through the boundary it leaves a dislocation $\mathbf{L}_I$ in the boundary whose Burgers vector is given by Equation 2. From Fig. 6 the rotation matrix a_{ij} is represented by

$$a_{ij} = \begin{bmatrix} \cos\theta & -\sin\theta & 0 \\ \sin\theta & \cos\theta & 0 \\ 0 & 0 & 1 \end{bmatrix} \tag{18}$$

and is identical to the one obtained for a tilt boundary. From Equations 2 and 18, the Burgers vector of the interface dislocation is given by

$$\boldsymbol{b}_I = [(b_1 - b_2 \cos\theta), b_2 \sin\theta, 0] \,. \tag{19}$$

For a symmetric tilt $\mathbf{n}_I$ is given by

$$\mathbf{n}_I = (\cos\theta/2, -\sin\theta/2, 0) \tag{20}$$

and for an asymmetric tilt, $\mathbf{n}_I$ is given by

$$\mathbf{n}_I = (\cos\alpha, -\sin\alpha, 0) \,. \tag{21}$$

If $\boldsymbol{b}_1$ is equal to $\boldsymbol{b}_2$ Equation 19 reduces to

$$\boldsymbol{b}_I = b_1 [(1 - \cos\theta), \sin\theta, 0] \tag{22}$$

which is the same result as that obtained for a simple tilt boundary. If the boundary is one of symmetric tilt, then from Equations 20 and 22, Equation 4 is satisfied and the interface dislocation is of glissile type [19]. However, for asymmetric tilt boundaries as well as when $\boldsymbol{b}_1$ is not equal to $\boldsymbol{b}_2$, Equation 4 will not be satisfied since the Burgers vector of the interface dislocation does not lie in the boundary. When $\theta = 0$,

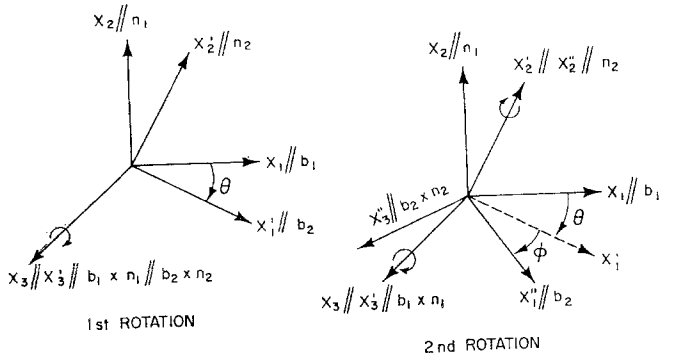

Figure 7 Sequence of rotations and the relationships between the co-ordinate axes.

$\boldsymbol{b}_I$ will be zero only if $\boldsymbol{b}_1$ is equal to $\boldsymbol{b}_2$, otherwise, $\boldsymbol{b}_I$ will be the difference between $\boldsymbol{b}_1$ and $\boldsymbol{b}_2$. The result for $\theta = 0$, is identical to that obtained by Fleischer [15]. Fig. 6 shows the orientation of $\boldsymbol{b}_I$ for different orientations of the slip systems in the two phases adjacent to the boundary.

In Fig. 6, the interface dislocations are of pure edge type and they are defined as glissile or sessile with reference to the original plane of the boundary before deformation. For a homogeneous shear, however, the boundary acquires an asymmetry owing to the formation of ledges such as represented in Fig. 3b. With reference to this asymmetric plane of the boundary, the array of boundary dislocations obtained as a result of the homogeneous shear for all of the orientations of the slip systems discussed in Fig. 6 can be resolved into two arrays of edge dislocations represented by Fig. 3e and f. From the previous discussion, it is clear that the homogeneous shear would increase the angle of tilt by an amount $\Delta\theta$ given by Equation 11. On the other hand, the long range stress fields associated with the dislocation arrays can be relieved by nucleation of crystal lattice dislocations which, for Fig. 6a, increase the asymmetry but changes the misorientation angle back to θ. For Fig. 6d, however, the stress fields associated with the interface dislocations could be annihilated by the nucleation of misfit dislocations from either phase which brings the orientation back to zero tilt. As a result of the homogeneous shear and the subsequent stress relief process, the interface acquires an asymmetry owing to the ledges along the boundary.

In a further more generalized case, we remove the constraint that $\mathbf{x}_3$ and $\mathbf{x}_3'$ are parallel and instead cause additional rotation of the co-ordinates by an angle, ϕ, with respect to the n_2 axis as shown in Fig. 7. The transformation matrix for the second rotation is given by

$$a_{ij}' = \begin{bmatrix} \cos\phi & 0 & \sin\phi \\ 0 & 1 & 0 \\ -\sin\phi & 0 & \cos\phi \end{bmatrix} \qquad (23)$$

and the total transformation (the order of rotation being first, $\theta°$ around $\mathbf{x}_3$ axis and then, ϕ around n_2 axis) is given by the product of a_{ij} and a_{ij}'.

$$A_{ij} = \begin{bmatrix} \cos\phi\cos\theta & -\cos\phi\sin\theta & \sin\phi \\ \sin\theta & \cos\theta & 0 \\ -\cos\theta\sin\phi & \sin\theta\sin\phi & \cos\phi \end{bmatrix} \qquad (24)$$

Equation 24 can easily be checked for $\phi = 0$ when A_{ij} reduces to a_{ij} given by Equation 18.

The Burgers vector of the boundary dislocation can now be determined if an edge dislocation which is parallel to the $\mathbf{x}_3$ axis (parallel to the first rotation axis) passes through the boundary. From Equations 2 and 24, $\boldsymbol{b}_I$ is given by

$$\boldsymbol{b}_I = [(b_1 - b_2\cos\phi\cos\theta), \; b_2\cos\phi\sin\theta, \; -b_2\sin\phi]. \qquad (25)$$

For $\phi = 0$ Equation 25 reduces to Equation 19. Equation 25 shows that in addition to the edge components discussed with reference to Fig. 6, $\boldsymbol{b}_I$ will now have screw components since the $\boldsymbol{x}_3$ component in Equation 25 is not zero.

For the case where $\theta = 0$ and $\phi \neq 0$ Equation 24 reduces to Equation 23 and Equation 25 reduces to

$$\boldsymbol{b}_I = [(b_1 - b_2\cos\phi), \; 0, \; -b_2\sin\phi] \; . \qquad (26)$$

If the rotation is symmetric then $\mathbf{L}_I$ will be given by

$$\mathbf{L}_I = [-\sin\phi/2, \; 0, \; \cos\phi/2] \; . \qquad (27)$$

For an edge dislocation (Fig. 6) passing through the boundary (the line vector of the dislocation is now perpendicular to the rotation axis n_2) the Burgers vector of the interface dislocation is given by Equation 26. It can be easily shown that for a symmetric rotation and for $\boldsymbol{b}_1 = \boldsymbol{b}_2$, $\boldsymbol{b}_I \times \mathbf{L}_I = 0$ showing that the interface dislocation will be a pure screw [19]. However, for a general case the interface dislocation is of mixed type as illustrated in Fig. 8.

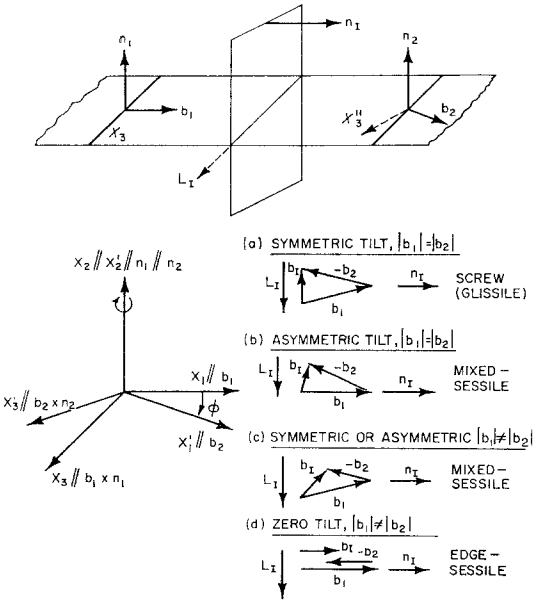

Figure 8 Passage of perpendicular edge dislocations from phase I to phase II and characteristics of the resulting interface dislocations for various orientations of the slip systems when $\theta = 0$.

As a result of the homogeneous shear for various orientations of the slip system discussed in Fig. 8, the boundary again acquires an asymmetry similar to that described in Fig. 3. The array of dislocations corresponding to the orientation in Fig. 8a is similar to an array of pure screw dislocations represented in Fig. 3d. The long range stress fields of this array can be relieved by nucleating CLD in both phases which combine at the boundary to give interface dislocations the Burgers vectors of which are opposite to that represented in Fig. 8a. Alternately, the stress fields could also be relieved by nucleating the CLD in both phases, the combination of which gives rise to an array of screw interface dislocations that are orthogonal to the one generated by homogeneous shear. It is to be noted that the crystal lattice dislocations from both phases may be needed to relieve the stress field of the arrays of the interface dislocations generated as a result of the homogeneous shear [32]. The dislocation arrays corresponding to Fig. 8b and c, on the other hand, can be resolved into an array of screw dislocations such as in Fig. 3d and an array of edge dislocations, such as in Fig. 3f. While the edge dislocation array has no long range stress fields, the stress fields of the array of screw dislocations can be relieved by the processes discussed above.

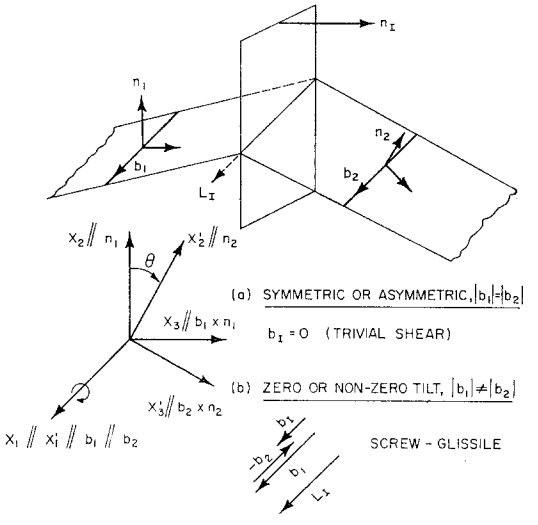

Figure 9 Passage of parallel screw dislocations from phase I to phase II and the characteristics of the resulting interface dislocations for various orientations of the slip systems in the two phases.

6.2. Screw dislocations

We will now consider the nature of the boundary dislocations resulting from the passage of screw dislocations through the boundary. As a first step, consider the rotation axis similar to that shown in Fig. 6 and the line vector parallel to the rotation axis. Fig. 9 shows the orientation of the slip system and the dislocation as well as the resulting Burgers vector for different cases. The rotation matrix for such orientation of the co-ordinates is given by

$$a_{ij} = \begin{bmatrix} 1 & 0 & 0 \\ 0 & \cos\theta & -\sin\theta \\ 0 & \sin\theta & \cos\theta \end{bmatrix} \qquad (28)$$

Equation 28 differs from Equation 18 owing to the differences in the system of co-ordinate axes

represented in Figs. 6 and 9. From Equations 2 and 28, $\boldsymbol{b}_{\mathrm{I}}$ is given by

$$\boldsymbol{b}_{\mathrm{I}} = \boldsymbol{b}_1 - \boldsymbol{b}_2 \ . \tag{29}$$

For $\boldsymbol{b}_1 = \boldsymbol{b}_2$, $\boldsymbol{b}_{\mathrm{I}}$ will be zero and the result is identical to that obtained by Das and Marcinkowski [19]. For $\boldsymbol{b}_1 \neq \boldsymbol{b}_2$ a screw dislocation is left at the boundary. An array of such dislocations will have a long range stress field associated with it.

However, if we introduce an additional rotation ϕ about the n_2 axis (similar to Fig. 7) Equation 28 will change to

$$A_{ij} = \begin{bmatrix} \cos\phi & -\sin\phi\sin\theta & -\sin\phi\cos\theta \\ 0 & \cos\theta & -\sin\theta \\ \sin\phi & \sin\theta\cos\phi & \cos\phi\cos\theta \end{bmatrix} . \tag{30}$$

Equation 30 reduces to Equation 28 for $\phi = 0$ or to Equation 23 for $\theta = 0$.

From Equations 2 and 30, a passing screw dislocation will leave a dislocation at the boundary with a Burgers vector given by

$$\boldsymbol{b}_{\mathrm{I}} = [(b_1 - b_2\cos\phi), \quad b_2\sin\phi\sin\theta, b_2\sin\phi\cos\theta]. \tag{31}$$

For $\phi = 0$, Equation 31 reduces to Equation 30. For $\theta = 0$ and for $\phi \neq 0$, the glide dislocations considered in Fig. 9 is perpendicular to the rotation axis n_2. Equation 31 for this case reduces to

$$\boldsymbol{b}_{\mathrm{I}} = [(b_1 - b_2\cos\phi), 0, b_2\sin\phi] \ . \tag{32}$$

Fig. 10 shows the various orientations of the two slip systems and the resulting interface dislocations. For the orientation of the two slip systems corresponding to Fig. 10a, the array of interface dislocations as a result of the homogeneous shear would correspond to that of Fig. 3e. Contrary to the previous assertion [19], no stress relief process is necessary since the array has no long range stress fields. The dislocation array, however, induces an additional tilt component given by Equation 11. For Fig. 10d, as well as for Fig. 9b, homogeneous shear would result into an array of screw interface dislocations and unlike the array corresponding to Figs. 6d and 8d, the stress field of this array is not relieved by prismatic misfit dislocations since there are no dilatational stress fields for an array of screw dislocations. The stress fields could, however, be relieved by an equivalent orthogonal set of screw-type interface dislocations that have to be generated by the combination of CLD from both phases. Such an orthogonal set of screw dislocations, however, induces a twist

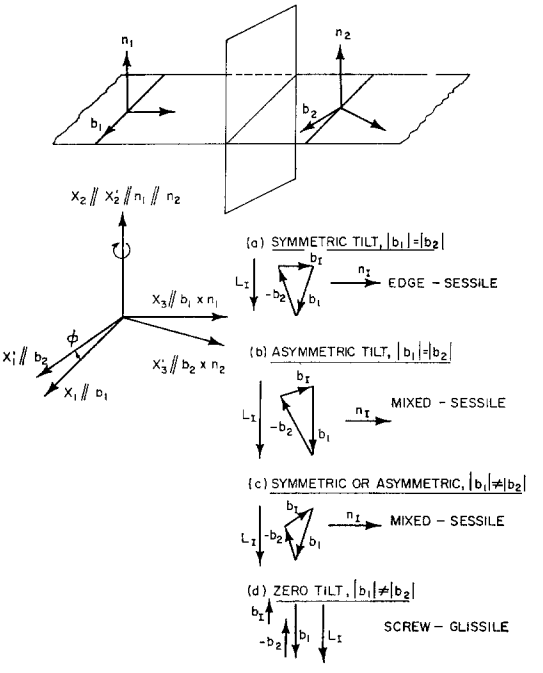

Figure 10 Passage of perpendicular screw dislocations from phase I to phase II and the characteristics of the resulting interface dislocations for various orientations of the slip systems in the two phases.

component in the boundary. Alternately, the stress fields could be relieved by generating a parallel array of screw-type interface dislocations the Burgers vectors of which are opposite to those of the dislocations resulted owing to the homogeneous shear.

The nature of interface dislocations resulting from the passage of CLD across the interface has already been discussed for the case where γ (Fig. 4) is zero. However, the dislocation could also pass through the boundary when γ is not zero. To illustrate this, consider a system of co-ordinates represented in Fig. 11 where the axis of rotation is parallel to $\mathbf{n}_{\mathrm{I}}$. The transformation matrix for this case is given by

$$a_{ij} = \begin{bmatrix} \cos\gamma & \sin\gamma & 0 \\ -\sin\gamma & \cos\gamma & 0 \\ 0 & 0 & 1 \end{bmatrix} \tag{33}$$

and from Equation 2 the Burgers vector of an interface dislocation arising from the passage of the screw dislocation represented in Fig. 11 is given by

$$\boldsymbol{b}_{\mathrm{I}} = [(b_1 - b_2\cos\gamma), -b_2\sin\gamma, 0] \ . \tag{34}$$

Since $\mathbf{n}_{\mathrm{I}}$ is the axis of rotation (parallel to $\mathbf{x}_3$)

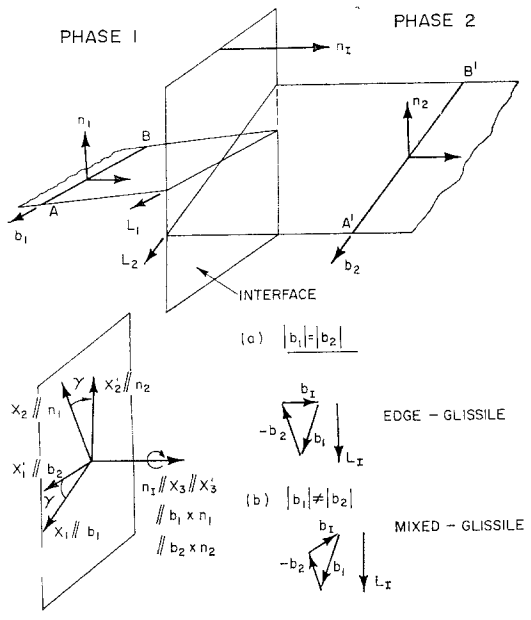

Figure 11 Passage of a screw dislocation from phase I to phase II when slip planes adjacent to the interface are in a twisted orientation.

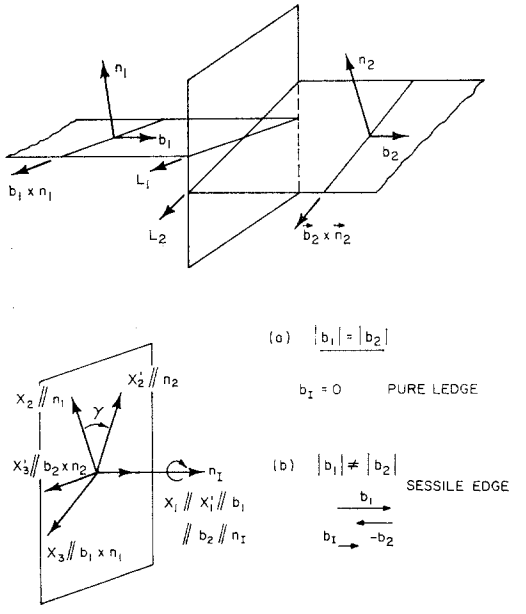

Figure 12 Passage of an edge dislocation by climb from phase I to phase II when slip planes adjacent to the interface are in a twisted orientation.

its co-ordinates are (001). Hence, from Equation 34 the interface dislocation will be glissile whether or not $\boldsymbol{b}_I = \boldsymbol{b}_2$. Fig. 11 shows that the two slip planes are twisted by an angle γ with respect to each other. This does not necessarily mean that the interface is a twist boundary. (Even for a simple tilt boundary γ may not be zero if one considers two different slip systems adjacent to the boundary.) If a dislocation AB is converted to A′B′ (Fig. 11), in addition to creating the interface dislocation described by Equation 34, the dislocation has to glide by an angular component γ. For $\gamma = 0$, Equation 34 reduces to Equation 29. The homogeneous shear would leave an array of dislocations such as in Fig. 3f for the orientation of b_I represented in Fig. 11a and a combination of arrays given by Fig. 3d and f for the orientation of b_I represented in Fig. 11b, all arrays having long range stress fields. When γ is not zero, either twist disclination loops or diffusion of point defects are needed for the dislocations that have Burgers vector component along $\mathbf{n}_I$ to be channelled through the boundary. The details of the mechanism of channelling of the dislocations by a twist disclination loop has been discussed earlier [20]. Fig. 12, on the other hand, shows the defects left by the crystal dislocation as it moves from one phase to the other by climb. For the case when $\boldsymbol{b}_1 = \boldsymbol{b}_2$ no interface dislocation is left behind. However, from Equation 5 a dislocation free ledge is left behind. Hence homogeneous shear would induce an asymmetry in the twist boundary. On the other hand, when $\boldsymbol{b}_1 \neq \boldsymbol{b}_2$ an edge dislocation similar to that shown in Fig. 6d is left behind along with the ledges.

7. Summary and conclusions

The deformation of internal boundaries such as grain boundaries, twin boundaries, two-phase interfaces, etc, has been analysed using the concepts of grain-boundary dislocations. In particular, attention has been focused on the disturbance created at the boundary when a glide dislocation crosses the boundary. Such a disturbance is characterized by a boundary dislocation, the nature of which can be determined from a knowledge of the orientation relationships between the slip systems adjacent to the boundary. In fact, Burgers vectors of all of the dislocations associated with all of the internal boundaries can be represented by a single expression given by Equation 2. Physically, Equation 2 describes the principles of conservation of the Burgers vector for a dislocation and it can be used to interpret the Burgers vectors of dislocations in internal boundaries as either the

TABLE I

Orientation of slip systems			Glide dislocations			Case	Boundary dislocation			
Rotation axis	Rotation angle*	Type	Type	Line vector	Burgers vector		Type	Line vector	Burgers vector	Mobility
x_3-axis	θ	Tilt	Parallel edge†	x_3-axis	[100]	(a) Symmetric tilt, $b_1 = b_2$	Edge	x_3-axis	b_1 [(1 − cos θ), sin θ, 0]	Glissile
						(b) Asymmetric tilt, $b_1 = b_2$	Edge	x_3-axis	b_1 [(1 − cos θ, sin θ, 0]	Sessile
						(c) Symmetric or asymmetric tilt, $b_1 \neq b_2$	Edge	x_3-axis	[($b_1 - b_2 \cos\theta$)), $b_2 \sin\theta$, 0]	Sessile
						(d) Zero tilt, $b_1 \neq b_2$	Edge	x_3-axis	[$b_1 - b_2$, 0, 0]	Sessile
$n_1 = n_2$ axis	ϕ	Tilt	Perpendicular edge	x_3-axis	[100]	(a) Symmetric tilt, $b_1 = b_2$	Screw	$\left[-\sin\frac{\phi}{2}, 0, \cos\frac{\phi}{2}\right]$	b_1 [(1 − cos ϕ), 0, − sin ϕ]	Glissile
						(b) Asymmetric tilt, $b_1 = b_2$	Mixed	?	b_1 [(1 − cos ϕ), 0, −sin ϕ]	Sessile
						(c) Symmetric or asymmetric tilt, $b_1 \neq b_2$	Mixed	?	[$b_1 - b_2 \cos\phi$, 0, − b_2 sin ϕ]	Sessile
						(d) Zero tilt, $b_1 = b_2$	Edge	x_3-axis	[$b_1 - b_2$, 0, 0]	Sessile
x_3-axis and n_2-axis	θ and ϕ	Complex tilt	Mixed edge	x_3-axis	[100]	(a) Symmetric tilt, $b_1 = b_2$	Mixed		b_1 [(1 − cos θ cos ϕ), θ, − sin ϕ]	Glissile
						(b) Asymmetric tilt, $b_1 = b_2$	Mixed	?	b_1 [(1 − cos 1 cos ϕ), cos 1 sin 1, − sin ϕ]	Sessile
						(c) Symmetric or asymmetric tilt, $b_1 \neq b_2$	Mixed	?	[$b_1 - b_2 \cos\phi \cos\theta$, $b_2 \cos\phi \sin\theta - b_2 \sin\phi$]	Sessile
x_3-axis and n_2-axis	θ and ϕ	Complex tilt	Mixed edge	x_3-axis	[100]	(d) Zero tilt, $b_1 = b_2$	Edge	x_3-axis	[$b_1 - b_2$, 0, 0]	Sessile
x_1-axis	θ	Tilt	Parallel screw	[100]	[100]	(a) Symmetric or asymmetric tilt, $b_1 = b_2$	Trivial shear			
						(b) Zero or non-zero tilt, $b_1 \neq b_2$	Screw	x_1-axis	[$b_1 - b_2$, 0, 0]	Glissile
$n_1 = n_2$ axis	ϕ	Tilt	Perpendicular screw	[100]	[100]	(a) Symmetric tilt, $b_1 = b_2$	Edge	[cos ϕ/2, 0, sin ϕ/2]	b_1 (1 − cos ϕ, 0, sin ϕ)]	Sessile
						(b) Asymmetric tilt, $b_1 = b_2$	Mixed	?	b_1 (1 − cos ϕ, 0, sin ϕ)]	Sessile
						(c) Symmetric or asymmetric tilt, $b_1 \neq b_2$	Mixed	?	[$b_1 - b_2 \cos\phi$, 0, $b_2 \sin\phi$]	Sessile
						(d) Zero tilt $b_1 \neq b_2$	Screw	x_1-axis	[$b_1 - b_2$, 0, 0]	Glissile
x_2-axis and n_2-axis	θ and ϕ	Complex tilt	Mixed screw	[100]	[100]	(a) Symmetric tilt, $b_1 = b_2$	Edge	?	b_1 [1 − cos ϕ, sin ϕ sin θ, sin ϕ cos θ]	Sessile
						(b) Asymmetric tilt, $b_1 = b_2$	Mixed	?	b_1 [1 − cos ϕ, sin ϕ sin θ, sin ϕ cos θ]	Sessile
						(c) Symmetric or asymmetric tilt, $b_1 \neq b_2$	Mixed	?	[$b_1 - b_2 \cos\phi$, $b_2 \sin\phi$ sin θ b_2 sin ϕ cos θ]	Sessile
x_3-axis and n_2-axis	θ and ϕ	Complex tilt	Mixed screw	[100]	[100]	(d) Zero tilt $b_1 \neq b_2$	Screw	x_1-axis	[$b_1 - b_2$, 0, 0]	Glissile
x_3-axis parallel to n_1-axis	γ	Twist	Screw	[100]	[100]	(a) $b_1 = b_2$	Edge	[cos γ/2, sin γ/2, 0]	b_1 [1 − cos γ, − sin γ, 0]	Glissile
						(b) $b_1 \neq b_2$	Edge	[cos γ/2, sin γ/2, 0]	[$b_1 - b_2$ cos γ, $-b_2$ sin γ, 0]	Glissile
	γ	Twist	Edge	[100]	[100]	(a) $b_1 = b_2$	Diffusion or twist disclination loop needed.			
						(b) $b_1 \neq b_2$	Diffusion or twist disclination loop needed. Ledge with a sessile edge dislocation left behind.			

*The angles θ and ϕ give the orientation relationships between the slip systems adjacent to the interface (ref. Fig. 7).
†The glide dislocations are defined as parallel or perpendicular dislocations with reference to the rotation axis.

sum or the difference of the Burgers vectors of the CLD of the two phases adjacent to the boundaries.

Among other things, it is also shown that the orientation and shape of the boundaries are altered as a result of a homogeneous shear. Such a shear also leaves an array of dislocations that may have long range stress fields which could be relieved by the nucleation of CLD in both phases. The nature of the interface dislocations produced as a result of the passage of a dislocation through the boundary is derived for some simple orientations and is summarized in Table I.

Acknowledgements

The authors would like to express their thanks to Dr E. S. P. Das, now with the Materials Science Division of Argonne National Laboratory, Mr Wen Feng Tseng, now with the Chemical Engineering Department of the University of Delaware and Dr W. H. Cullen, Jun., now with the OTD Division of the Naval Research Laboratories for a number of helpful discussions. The present research effort was supported by the National Science Foundation under Grant No. GH-32262.

References

1. I.M.D. Symposium on "Deformation and Strength of Polycrystals", Vol. 1 (Met. Trans., 1970).
2. R. CLARK and B. CHALMERS, *Acta Metallurgica* **2** (1954) 80.
3. K. AUST and N. CHEN, *ibid* **2** (1954) 632
4. R. DAVIS, R. L. FLEISCHER, J. D. LIVINGSTONE and B. CHALMERS, *J. Metals* **9** (1957) 136.
5. J. D. LIVINGSTONE and B. CHALMERS, *Acta Metallurgica* **5** (1957) 322.
6. R.L.FLEISCHER and B. CHALMERS, *Trans. Met. Soc. AIME* **212** (1958) 265.
7. J. J. HAUSER and B. CHALMERS, *Acta Metallurgica* **2** (1961) 802.
8. R. E. HOOK and J. P. HIRTH, *ibid* **15** (1967) 535.
9. J. J. GILMAN, *ibid* **1** (1953) 426.
10. T. KAWADA, *J. Phys. Soc. Japan* **6** (1951) 362.
11. K. G. DAVIS, E. TEGNTSOONIAN and A. LU, *Acta Metallurgica* **14** (1966) 1677.
12. T. J. KOPPENAAL, *ibid* **10** (1962) 684.
13. L. J. BROUTMAN and R. H. KROCK (eds) "Modern Composite Materials" (Addison-Wesley, Reading, Mass., 1967).
14. H. E. CLINE, J. L. WALTER, E. F. KOCH and L. M. OSIKA, *Acta Metallurgica* **19** (1971) 405.
15. R. L. FLEISCHER, *ibid* **8** (1960) 598
16. M. J. MARCINKOWSKI, Conference on "Fundamental Aspects of Dislocation Theory" (edited by John A. Simmons, R. deWit and R. Bullough) NBS Special Publication No. 317, Washington, **1** (1970) 531.
17. M. J. MARCINKOWSKI and W. F. TSENG, *Met. Trans.* **1** (1970) 3397.
18. E. S. P. DAS and M. J. MARCINKOWSKI, *Mat. Sci. Eng.* **8** (1971) 189.
19. *Idem, Acta Metallurgica* **20** (1972) 199.
20. *Idem, J. Appl. Phys.* **42** (1971) 4107.
21. H. GLEITER and G. BÄRO, *Met. Sci. Eng.* **2** (1967) 229.
22. H. GLEITER, E. HORNBOGEN and G. BÄRO, *Acta Metallurgica* **16** (1968) 1053.
23. G. BÄRO, H. GLEITER and E. HORNBOGEN, *Mat. Sci. Eng.* **3** (1968) 92.
24. W. BOLLMANN, "Conference on the Fundamental Aspects of Dislocation Theory" (edited by John A. Simmons, R. deWit and R. Bullough) NBS Special Publication No. 317, Washington, **1** (1970).
25. F. F. LONGE, *Acta Metallurgica* **15** (1967) 311.
26. H. GOLDSTEIN, "Classical Mechanics" (Addison-Wesley, Reading. Mass, 1965).
27. B. CHALMERS, *J. Less Common Metals* **28** (1972) 277.
28. J. F. NYE, "Physical Properties of Crystals" (Oxford Press, London, 1957)
29. M. J. MARCINKOWSKI, "Electron Microscopy and Structure of Materials" (edited by G. Thomas, R. M. Fulrath and R. M. Fisher) (University of California, Berkeley, 1972) p. 382.
30. M. J. MARCINKOWSKI, A. J. BAKER and R. M. FISHER, *Phys. Stat. Sol.* **12a** (1971) 431.
31. K. SADANANDA and M. J. MARCINKOWSKI, *J. Appl. Phys.* (1973) in press.
32. *Idem, ibid.*
33. J. P. HIRTH and R. W. BALLUFFI, *Acta Metallurgica* **21** (1973) 929.
34. R. C. GIFKINS, *Met. Sci. J.* **1** (1973) 15.
35. R. L. BELL and T. G. LANGDON, in "Interfaces" (edited by R. C. Gifkins) (Butterworth, Sidney, 1969) p. 115.
36. R. N. STEVENS, *Met. Rev.* **11** (1966) 108.
37. T. G. LANGDON, *Met. Trans.* **3** (1972) 927.
38. J. C. M. LI, in "Electron Microscopy and Strength of Crystals" (edited by G. Thomas and J. Washburn) (Interscience, New York, 1963).
39. W. T. READ, "Dislocations in Crystals" (McGraw Hill, New York, 1953) p. 155.
40. M. J. MARCINKOWSKI, K. SADANANDA and WEN FENG TSENG, *Phys. Stat. Sol.* **a17** (1973) 423.
41. M. J. MARCINKOWSKI and K. SADANANDA, *ibid* **a18** (1973) 361.
42. WEN FENG TSENG, M. J. MARCINKOWSKI and E. S. DWARAKADASA, *J. Mater. Sci.* **9** (1974) 41.

Received 18 June and accepted 16 July 1973.